University of Calgary

undergraduate thesis project

Development of a desktop muon detector

Jordan Hanania

supervised by

Dr. Jason Donev

CONTENTS

ABSTRACT

Cosmic muons constantly bombard the Earth's surface, contributing to annual radiation doses in humans. Two small scintillator detectors were constructed from scratch, used for the purpose of muon detection. Experiments with these detectors investigated muon penetration in concrete and the theory of relativity, with positive results for each.

I. INTRODUCTION

This undergraduate thesis project for Physics 598 is centered around the development of two instruments used to detect cosmic muons, that are small enough to fit on the corner of a desk. These detectors were built from scratch following a thorough outline made by a group at MIT [2]. This project aimed at gaining experience with instrument development, calibration, and experimentation, while also producing two detectors that can be used for educational purposes after completion of the project.

This report will cover all aspects of the project, from the early stages of acquiring parts, to the finished product and experiments. Early sections discuss background information: an exploration into what muons are, methodology used in their detection, and theory of the detectors. The following sections will cover the steps taken in achieving operating detectors along with the calibration process. Finally, experiments will be analyzed with their results, and the future uses of the detectors will be discussed.

II. BACKGROUND

A. What is a muon?

Muons (μ) are fundamental particles in the lepton family. Other particles that are classified as leptons include the tauon, the electron, and three neutrinos: termed electron, muon, and tau neutrinos. As a lepton, the muon has a spin of 1/2 and is similar to the electron in that it shares the same fundamental charge of $e = 1.6 \times 10^{-19}$ C. Unlike the electron however, the muon is unstable and decays with a mean lifetime of $\tau = (2.1969811 \pm 0.0000022) \times 10^{-6}$ seconds [3]. The primary decay modes for muons are:

$$\mu^- \rightarrow e^- + \bar{\nu}_e + \nu_\mu \quad \text{(Muon)}$$

$$\mu^+ \rightarrow e^+ + \nu_e + \bar{\nu}_\mu \quad \text{(Antimuon)}$$

This project investigated muons created high up in Earth's atmosphere, known as "cosmic muons". Cosmic muons are produced when high energy cosmic particles such as protons smash into molecules in the upper atmosphere, producing a shower of various fundamental and composite particles, with an example shown in Figure 1.

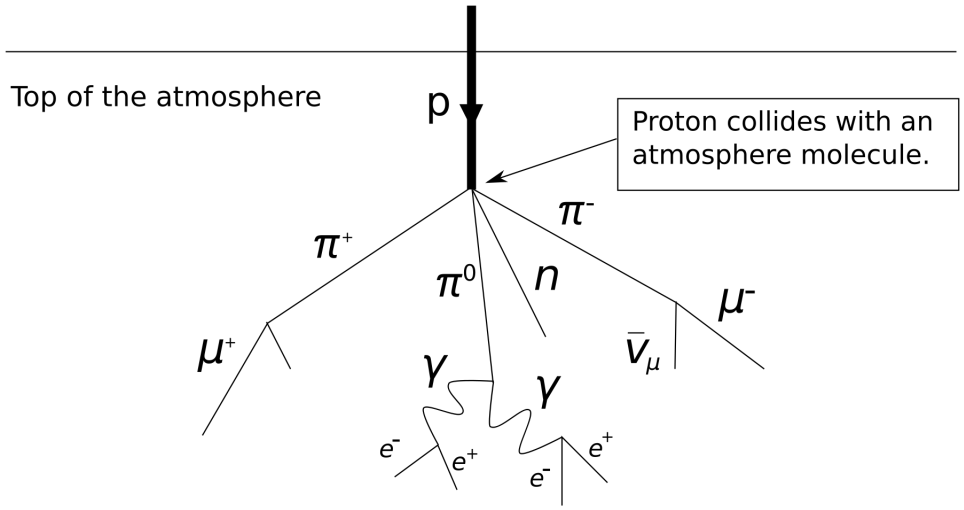

FIG. 1: Cosmic showers begin with a cosmic particle smashing into molecules in the atmosphere. This shower begins with a proton collision, producing pions π which quickly decay to muons μ (in around 26 nanoseconds). These muons then travel in approximately the same direction as the initial proton for us to detect on the ground [4].

B. What makes cosmic muons interesting?

1. Evidence for relativity

Cosmic muons have a history as being early experimental evidence for Einstein's Special Theory of Relativity. To see why, we will consider a muon's transit to Earth from both a classical and relativistic perspective.

Consider a muon produced in the upper atmosphere, at a height of $L_0 = 15 \times 10^3$ m above sea level, travelling at 99.9% of the speed of light ($v = 0.999c = 299492665\,\text{m/s}$).

Classically, the distance that this muon will travel is, on average,

$$d = v\tau_0 = 0.999c\left(2.197 \times 10^{-6}\text{s}\right) = 664.783\,\text{m}, \tag{1}$$

which is merely 4.4% of the length of the 15,000 m atmosphere.

Under the framework of relativity, the muon still decays in 2.197×10^{-6} s in its own frame. However, to an observer on the Earth, the muon's lifetime is much longer due to its relativistic velocity. The lifetime τ in the stationary Earth frame is thus dictated by the Lorentz factor, $\gamma = (1 - v^2/c^2)^{-1/2}$, which now becomes

$$\tau = \gamma\tau_0 = \frac{(2.197 \times 10^{-6}\text{s})}{\sqrt{1 - 0.999^2}} = 49.139 \times 10^{-6}\,\text{s}. \tag{2}$$

The distance that the relativistic muon travels in the Earth-bound observer's frame is then, on average,

$$d = v\tau = 0.999c\left(49.139 \times 10^{-6}\text{s}\right) = 14868.724\,\text{m}, \tag{3}$$

which is 99.1% of the length of the atmosphere. These numbers make the case for relativity very appealing, however observing a single muon on Earth is not evidence for relativity. This is because there is a non-zero probability P that the classical muon could still live 23 mean lifetimes and be detected on Earth (calculated to be $P = e^{-23} \approx 10^{-10}$ using Equation 4 below).

The way to test for relativistic effects is to measure muon counts at two different altitudes, and compare the results. If, within the same time interval, N_0 counts were measured at a height h above Earth's surface and N counts were measured on Earth's surface, then for an unstable particle with mean lifetime τ these counts are related by

$$\frac{N}{N_0} = \exp\left(-t/\tau\right), \tag{4}$$

where t is the time it takes for the muon to traverse the height h between detectors. The left side of Equation 4 is a measured constant, however the right side depends on whether a classical or relativistic perspective is taken. Consider first the classical case, where $t = h/v$. Equation 4 becomes:

$$\frac{N}{N_0} = \exp\left(-\frac{h}{v\tau_0}\right) \qquad \text{(classical)} \tag{5}$$

which can be rearranged to solve for the muon speed, given by

$$v_c = \frac{h}{\tau_0 \ln(N_0/N)}. \tag{6}$$

The experimenter operating under classical assumptions would then calculate the muon speed using Equation 6 to find that $v > c$, despite the speed of light being the universal speed limit [6]. Comparing data to the relativistic expression of Equation 7 however, derived by use of Equation 2 and 4, the experimenter should find consistency in their results.

$$\frac{N}{N_0} = \exp\left(-\frac{h\sqrt{1 - v^2/c^2}}{v\tau_0}\right) \qquad \text{(relativistic)} \tag{7}$$

This experiment was explored using the muon detectors built during this project, with results discussed in the *Experiments* section.

2. Muons as background radiation

Cosmic muons travel near the speed of light, and are able to ionize the atoms and molecules encountered within the human body. Cosmic radiation from muons and gamma rays contribute approximately 15% of the average human's natural radiation dose [7]. Due to the fact that muons are produced high in the atmosphere and decay on their path to Earth, people living at higher elevations will receive larger cosmic radiation doses. The typical dosage range from cosmic radiation annually is 0.3-1.0 milliSieverts, however pilots, astronauts, and frequent flyers will exceed this range [7].

C. Statistical methods in observing muons

The statistical distribution used in muon experiments is the "Poisson distribution". This distribution is used because muon events are independent of all previous events, there is an average muon count rate, and the probability of an event occurring is proportional to the time interval of detection, which are all defining properties of the Poisson

distribution [8]. The probability of observing r events in a time interval Δt in this distribution is

$$P(r) = \frac{(\lambda \Delta t)^r \, e^{-\lambda \Delta t}}{r!}, \tag{8}$$

where λ is the mean count rate of muons. The standard deviation σ of this distribution is

$$\sigma = \sqrt{\lambda \Delta t}, \tag{9}$$

which is the square root of the average number of counts μ measured in the time interval.

To illustrate the impact of Equation 8, the probability of observing exactly $r = 0, 1$, or 2 counts in a window of $t = 4$ seconds with a mean count rate $\lambda = 1$ count/sec is

$$\begin{aligned} P(0) &= \frac{(4)^0 \, e^{-4}}{0!} = 0.0183 \\ P(1) &= \frac{(4)^1 \, e^{-4}}{1!} = 0.0733 \\ P(2) &= \frac{(4)^2 \, e^{-4}}{2!} = 0.1465. \end{aligned} \tag{10}$$

The benefit of this distribution is the ease in which uncertainties in measured count number μ and count rate λ can be determined. Since the standard deviation is the square root of the number of counts, the count number with uncertainty, N, is

$$N = \mu \pm \sqrt{\mu} \tag{11}$$

and the count rate is

$$\lambda = \frac{\mu \pm \sqrt{\mu}}{t} \tag{12}$$

which allows one to minimize uncertainties by simply acquiring more counts. For this project, all trials aimed to acquire at least $\mu = 10,000$ counts per trial in order to keep the relative uncertainty below 1%.

III. THEORY OF THE DETECTOR

This project used scintillation detectors, which are some of the most widely used detection devices in nuclear and particle physics today [9]. The basic principle of these detectors is to make use of certain materials - known as scintillators - that emit photons when struck by a form of ionizing radiation. Early scintillators had to be analyzed by eye, which was a very inefficient and tedious process. Today scintillators can simply be coupled with a photomultiplier to detect their light. A photomultiplier (PM) is a device which works to convert the photons from the scintillator into an electric signal, which can then be processed by further circuitry. For this project, this circuitry is controlled by a microcontroller called an Arduino, which powers the circuit, measures signals, and outputs results to a computer.

A. The scintillator

As mentioned above, a scintillator is a material that emits photons when struck by a form of ionizing radiation. This fact alone is attractive to particle detection experiments, though there are other reasons that make a scintillation detector desirable, such as [9]:

1. **Sensitivity to Energy**. Scintillators are known to have a linear response in the amount of light they output to the energy of the incident particle, above a certain minimum energy. Coupled with a photomultiplier that exhibits a linear response to the light output, the final electric signal should have an amplitude proportional to the energy of the particle ($V_{PM} \propto E_\mu$). Although this proportionality is difficult to determine, the fact that it exists is enough to draw conclusions such as those made in the *Calibration* section later on.

2. **Fast Response Time**. Scintillators have a relatively high response and recovery time compared to other detectors. The time for the scintillator to emit light from a particle event and then recover is on the order of tens of nanoseconds, which allows scintillators to be used to good precision for high count rate experiments. Under the Poissonian distribution it is possible to determine how many counts are expected within a certain time, so the knowledge of recovery time allows for missed counts

to be corrected for. For our detectors, the count rates are sufficiently low enough that the probability of missing a count due to scintillator recovery time is negligible.

FIG. 2: Plastic scintillator in its initial condition, which was approximately 30cm x 30cm x 5.5cm in size.

The scintillator used in this experiment is a plastic scintillator, shown in Figure 2. Plastic is just one of the many types of scintillating mediums, with others including gases, glasses, organic liquids and crystals, and inorganic crystals. A plastic scintillator was used for this project becuase it is inexpensive and easily manipulated (cut, sanded, etc.).

B. The photomultiplier

The photomultiplier used in this project is a solid state Silicon Photomultiplier (SiPM), shown in Figure 3. It is 36 mm^2 in area and consists of 18,980 avalanche photodiodes.

The choice in using a SiPM over a traditional Photomultiplier Tube (PMT) in this project was twofold:

1. **Size**. The SiPM is a much smaller photodetector than a PMT. The goal of this project was to produce two small detectors that could be carried around easily and run just about anywhere, thus making the SiPM more practical.

2. **Low reverse bias voltage**. Compared to a PMT which needs on the order of kilovolts to operate, the SiPM only requires a reverse bias of 29.5 V. This bias is achieved by using a DC-DC booster, which provides a variable voltage output from a 5 volt power supply input.

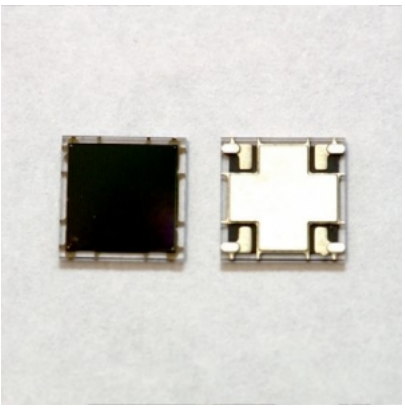

FIG. 3: Front and back view of the SiPM [10].

The SiPM functions as a photodetector when a reverse bias is applied over it. It is composed of avalanche photodiodes, each of which consist of an intrinsic (I) layer of silicon sandwiched between a negative (N) and positively (P) doped layer. Doping simply means that the silicon is combined with another atom in its crystal structure that either easily accepts electrons (P) or donates electrons (N). When the 29.5 V bias is applied over the photodiode, it attracts the charge carriers in the respective regions to the edge of the diode, creating a high electric field in the intrinsic region. This is shown in Figure 4.

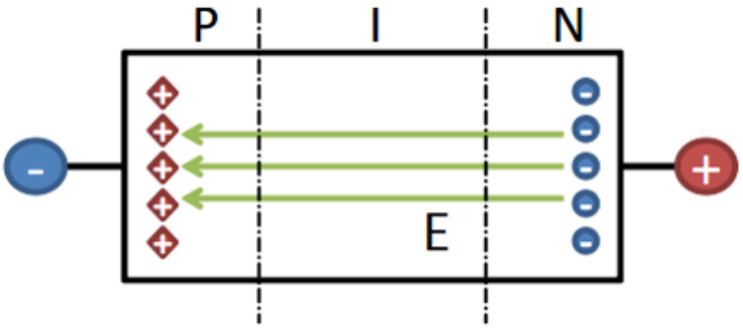

FIG. 4: A reverse biased PIN diode.

Now, when a photon of high enough energy ($\hbar\omega \geq E_{\text{bandgap,Si}}$) interacts with an electron in the intrinsic layer it may create an electron-hole pair, which will be forced to opposite ends due to the electric field. Not only will this electron-hole pair move, but since these charges experience large accelerations due to the high electric field, they will also produce new electron hole pairs in a process known as impact ionization. These newly produced electron-hole pairs produce more pairs, which go on to produce more, resulting in an

exponential increase in electron-hole pairs. This event is known as an avalanche, and is depicted in Figure 5. The gain from a single photon event can be as high as 10^7, which is how the SiPM can produce a measurable current from a photon event.

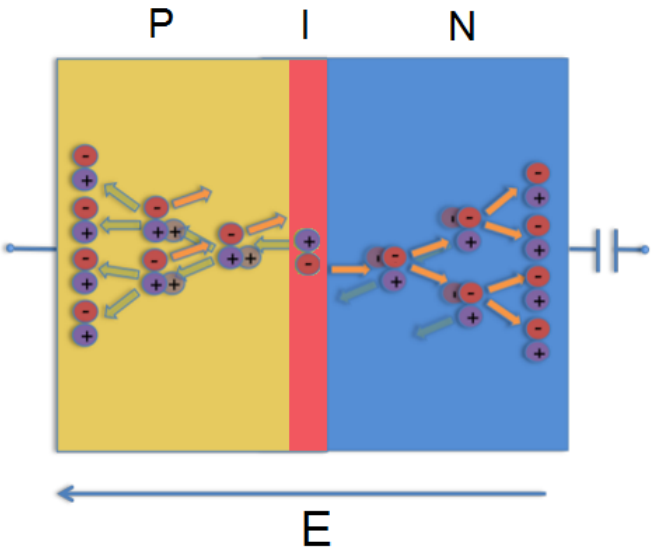

FIG. 5: An avalanche event in a PIN diode occurring from a photon detection [10].

C. Signal processing

After a muon has been detected through the combined scintillator-photomultiplier system, it is a matter of processing the SiPM signal in order to sample it properly and to register the event.

The first step in processing the SiPM signal is to amplify it. The SiPM signal is several millivolts, which cannot be registered by the Arduino microcontroller. In order to amplify this signal, we use a single-supply non-inverting operational amplifier, or non-inverting amplifier for short. The amplifier circuit is seen in Figure 6, with gain, A, given by $A = 1 + R_2/R_1$. Using the resistor values $R_2 = 57.6\,\text{k}\Omega$ and $R_1 = 1\,\text{k}\Omega$, the gain of the detectors in this project is approximately 58.6.

Following amplification, the signal is sent through a peak detecting circuit, shown in Figure 7. The purpose of this circuit is to determine the peak of the amplified signal so that the Arduino can measure it precisely. It works by using the input signal to charge

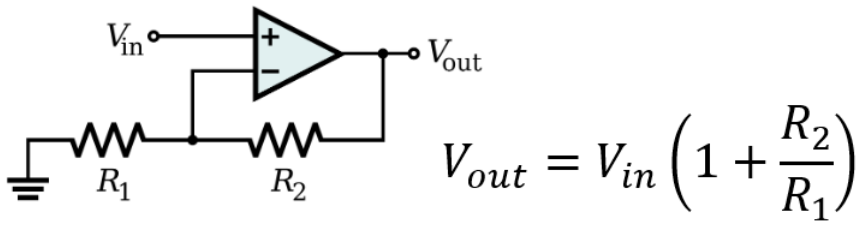

FIG. 6: Non-inverting op-amp circuit diagram with the relation between the SiPM signal (V_{in}) and amplified signal (V_{out}) [11].

up capacitor C_1 while the diodes are reverse biased. The use of the diode ensures that V_{out} is dictated by the charge on C_1 at any given time. The input signal from the amplifier peaks quite fast, so the capacitor is charged quickly and V_{out} becomes the peak value of that signal. The decay of this new signal is governed by the RC circuit formed by R_1 and C_1, with $V_{out}(t) = V_{out,0}\, e^{-t/\tau}$ where $\tau = C_1 R_1$. For our detector, $\tau = (1\text{nF})\,(100\text{k}\Omega) = 100\mu s$ which is enough time for the Arduino to determine the peak voltage. This $100\mu s$ contributes to detector deadtime, however it is not a considerable source of error on its own, as the probability of at least one event occurring in this time interval is: (Eq. 8) $P(r \geq 1, \Delta t = 100\mu s) = 1 - P(0, \Delta t = 100\mu s) = 1 - \exp(-100 \times 10^{-6}) = 0.0001$.

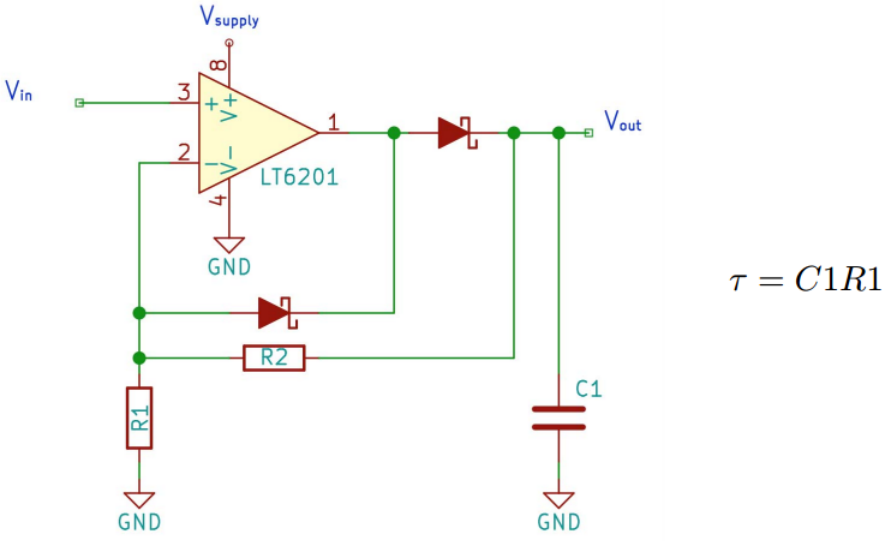

FIG. 7: Peak detecting circuit detects the peak of the amplified signal and holds this peak for long enough to be sampled by an Arduino [2].

IV. DETECTOR DEVELOPMENT

This section will outline the actual production of the two detectors. In order to detect muons simultaneously, two detectors were constructed for this project. This allows for simultaneous trials occurring at two altitudes, which as seen in the section IIB, can show some interesting physics. It also leaves the potential for the detectors to be eventually used as a muon telescope, similar to the Senior Physics Laboratory's Cosmic Ray Muon Telescope.

There are several components that are required in the building of these detectors, which have been tabulated in Appendix A. Most of these parts had to be ordered, however some of them were available through the physics department or were already owned. The bulk of this section will focus primarily on the detector production in the context of the *Theory of the Detector* section.

A. Machining the scintillator

The scintillator blocks were the first major pieces of the detectors that were produced. The scintillator was readily available from the physics department early on, which allowed for it to be machined while the ordered parts were being shipped.

The light proof aluminum containment box that the scintillator was to be placed in measured (12 x 9.4 x 5.7) cm while the initial piece of scintillator measured (30 x 30 x 5.5) cm, so the scintillator was cut down to size using a table saw. The saw had no difficulty getting through the material, however the scintillator in contact with the saw instantly melted leaving the faces extremely rough and deformed. Sanding and polishing of these surfaces was required because the scintillator faces needed to be very smooth in order to decrease light absorption at the boundaries. The polished scintillators were then covered in a clear coating, painted white, and wrapped in reflective aluminum tape. This increases reflectivity within the scintillator medium, while also preventing most external light from entering. A small window on the scintillator block was left uncovered in order to allow coupling to the photodetector.

(a) Birds-eye-view of the detector box.

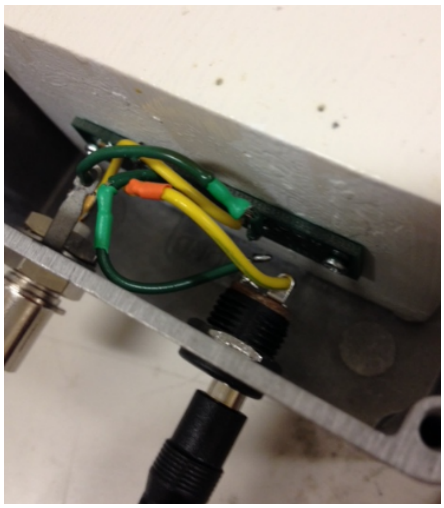

(b) Close-up of the SiPM board screwed onto the scintillator face.

FIG. 8: Inside of the detector box. Scintillator is the white block prior to adding reflective tape, with wire connections from the SiPM board to external electronics.

B. Assembling the circuitry

The next major part of building the detectors was to assemble the circuitry. The circuit boards were ordered from a local company, while all circuit components (listed in Appendix A) needed to be ordered online.

There are two required circuit boards for each detector, which are shown in Figure 9. The small rectangular boards hold the silicon photomultipliers (SiPMs) and several low-pass filters with a cut-off frequency of $f_{c/o} = (2\pi RC)^{-1} = 3.2\,\text{kHz}$. This acts to suppress noise from the power supply, which is of this order. The large square boards are the main circuitry boards, housing the micro-controller, power supply, amplifier, and peak detecting circuits. All boards required soldering many small surface mount components onto them.

Figure 10 shows the completed circuit boards for the first detector that was built. Minor improvements were made when assembling the second detector's circuitry (seen in Figure 11), which mainly includes using a pad mount DC jack and higher precision soldering. Overall, the circuit boards for both detectors function as expected with minor debugging having taken place.

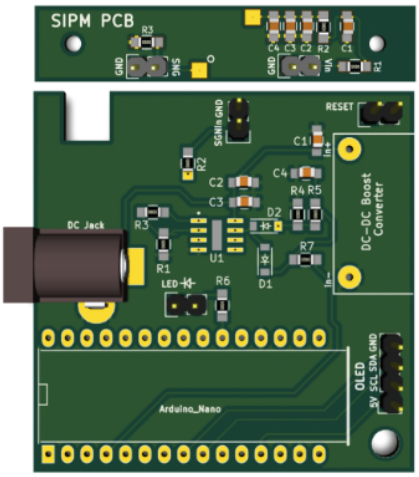

(a) Top side of the circuit boards.

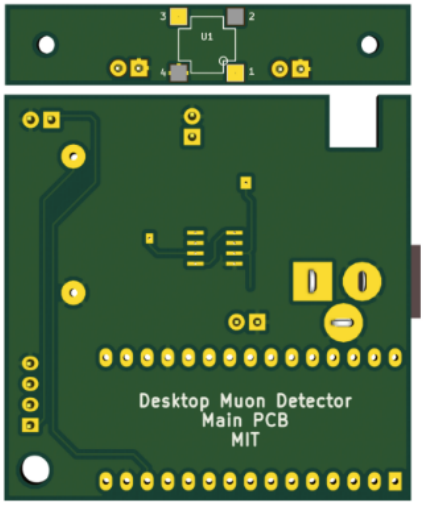

(b) Underside of circuit boards. SiPM is the only component on this side.

FIG. 9: Circuit boards created by the MIT group [2], which were used for this project.

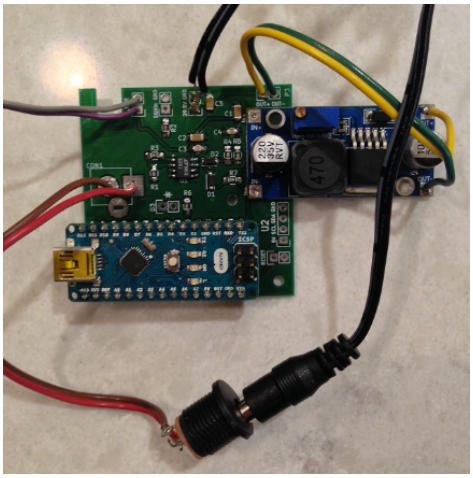

(a) Main circuit board. 5V power goes into the socket (red/brown cable) from either a wall plug or battery supply. This 5V is amplified to 29.5V with the overhanging DC-DC booster, which sets the reverse bias for the SiPM circuit.

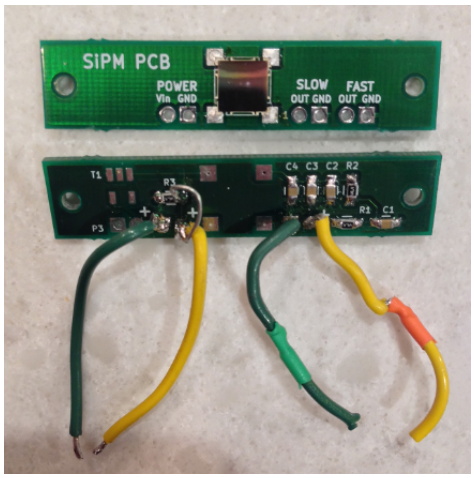

(b) SiPM circuit. Filters are used regulate the 29.5V power signal. Muon signals are sent out of the SLOW output.

FIG. 10: Finished circuit boards for one of the detectors.

The completed Main circuit boards are housed in old unused WiFi modems which provide a nice foundation for the entire detector unit. This is seen in Figure 11, which shows the second detector's main circuit board.

The SiPM boards are housed within the light proof aluminum enclosure, as seen in

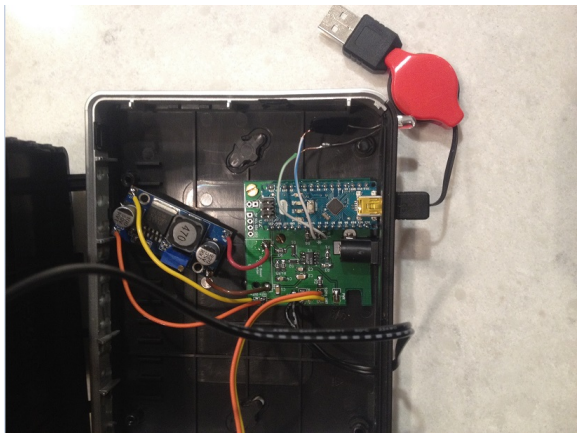

FIG. 11: Main circuit board for the second detector is screwed into an old WiFi modem, with external ports accessible through an opening in the back.

Figure 8. Before mounting the SiPM boards to the scintillator, clear high-vacuum grease was applied to the window in order to smooth the transition in refractional indices for the scintillator-air-glass interface [9]. This helps to maximize the transmission of light from the scintillator to the photodetector [12]. The SiPM boards were then screwed in place.

FIG. 12: The finished detectors (first built on left, second built on right).

C. Calibration and Testing

The first detector built was tested immediately upon its completion. It was quickly apparent that the SiPM board produced signals that would be expected from muon events, with pulse heights of 10-100 mV and decay times of ~ 500 ns as shown in Figure 13.

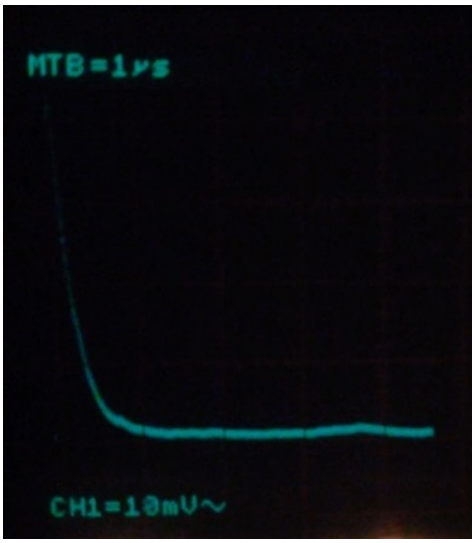

FIG. 13: Detected muon pulse seen on an oscilloscope. The background scale was dimmed in order to see the signal, however this pulse is around 50-70mV.

Both detectors were calibrated upon completion. The calibration method uses the signal proportionality mentioned in Section IIIA, in which it was said that the signal output by the SiPM is linearly proportional to the energy of the incident particle. For higher energy particles, more light will be produced within the scintillator, and therefore a higher amplitude pulse will be produced by the SiPM. Although the proportionality cannot be determined easily, it can be used to distinguish between high energy cosmic muons (kinetic energy ~ 2000 MeV) and gamma rays (~ 1 MeV).

Calibration was done using the Cosmic Ray Muon Telescope (CRMT) on the top floor of the Science B building. The CRMT was set to detect particles while its threshold voltage was varied, which determined how high a pulse needed to be in order to count as an event. Counts were accumulated at different threshold values and plotted, with results shown in Figure 14. Since the pulse heights are proportional to particle energy, the plot is essentially a cumulative distribution of the muon energies, with a clear plateau where one leaves the muon regime and begins to detect lower energy gamma rays.

Extensive data was then taken with the CRMT with high certainty. $N = 2219812 \pm 1490$

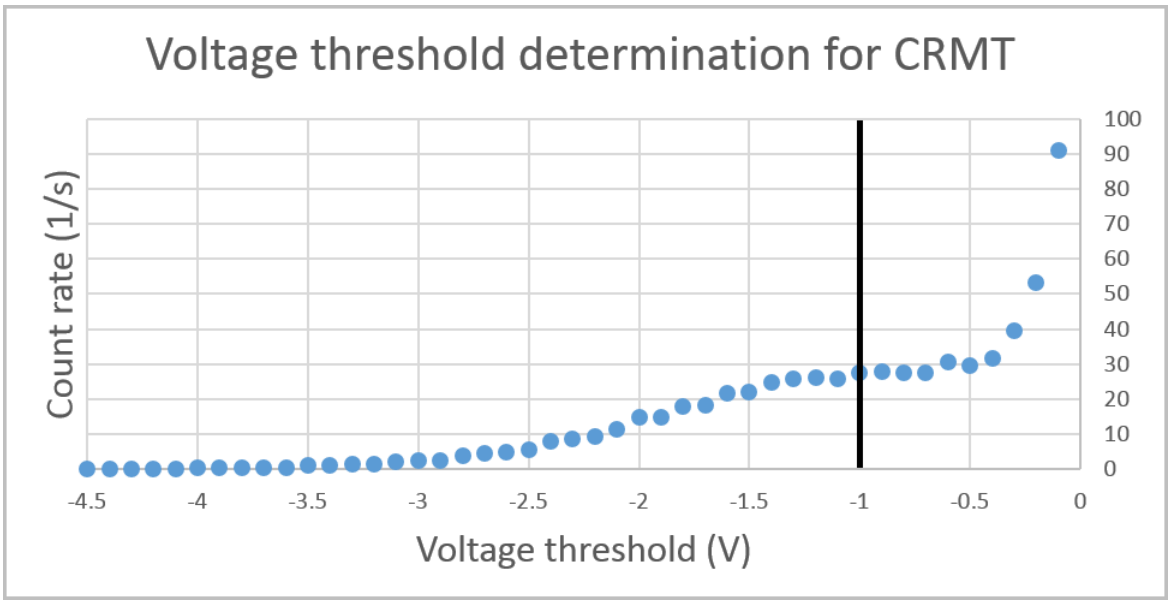

FIG. 14: Threshold determination shows stricter thresholds increasing negatively. This builds a cumulative plot of the muons until a plateau is reached, at which the threshold value is determined, shown by the vertical black line at −1 V.

counts were accumulated over a period of $\Delta t = 95665$ seconds. The detector area has dimensions (39.8 ± 0.2 cm) x (24.5 ± 0.4 cm), which corresponds to an area of 975.1 ± 16.7 cm^2. Thus the flux measured by the detector is

$$\Phi = \frac{N}{A\Delta t} = \frac{2219812 \pm 1490 \text{ counts}}{(975.1 \pm 16.7\,\text{cm}^2)\,(95665\,\text{s})} = (23.8 \pm 0.4) \times 10^{-3}\,\frac{\text{counts}}{\text{cm}^2 \cdot \text{s}}. \tag{13}$$

The goal was then to calibrate our detectors to the CRMT. This was done by varying the threshold voltages available to our detectors, until each detector's flux matched within uncertainty of the CRMT. Detector 1 had an area of $A_1 = (65.3 \pm 0.6)$ cm^2 and accumulated a count rate of $\lambda_1 = 1.54 \pm 0.03$ counts/sec, giving a flux of $\Phi_1 = (23.6 \pm 0.5) \times 10^{-3}$ counts/s/cm^2. Detector 2 had an area of $A_2 = (63.8 \pm 0.6)$ cm^2 and accumlated a count rate of $\lambda_2 = 1.51 \pm 0.03$ counts/sec, with a flux of $\Phi_2 = (23.7 \pm 0.5) \times 10^{-3}$ counts/s/cm^2.

After independent calibration, the detectors were left to run side by side at a different location than where they were calibrated, to test whether they were consistent with one another. These results are shown in Figure 15, with the basement trial detector 1 flux of $\Phi_{1B} = (20.4 \pm 0.2) \times 10^{-3}$ count/sec/cm^2 and detector 2 flux of $\Phi_{2B} = (20.5 \pm 0.2) \times 10^{-3}$ count/sec, and the middle floor trial detector 1 flux $\Phi_{1M} = (20.5 \pm 0.2) \times 10^{-3}$ count/sec/cm^2

and detector 2 flux $\Phi_{2M} = (20.7 \pm 0.2) \times 10^{-3}$ count/sec/cm^2

FIG. 15: Simultaneous side by side trial with both detectors shows that they fluctuate about the same mean flux, within error (Note: with units of 15 minutes^{-1} rather than seconds^{-1} in order to smooth the fluctuations).

V. EXPERIMENTS

The primary experiment set out to detect muons at different elevations, in attempts to verify the relativistic theory outlined in Section IIA. Detector 1 was placed beside the CRMT on the top floor of Science B (SB), while detector 2 was placed in the undergrad physics workroom in the basement of Science Theatres (ST). They were then left to collect data for several hours until the $N > 10,000$ counts were accumulated, which is shown in Figure 16.

The relativity argument from Section IIA predicts that the counts should be very close to one another ($N_0 = 0.995N$), however the measured counts differed significantly. These counts were taken within the same time period in upstairs SB (N_0) and downstairs ST (N), and were:

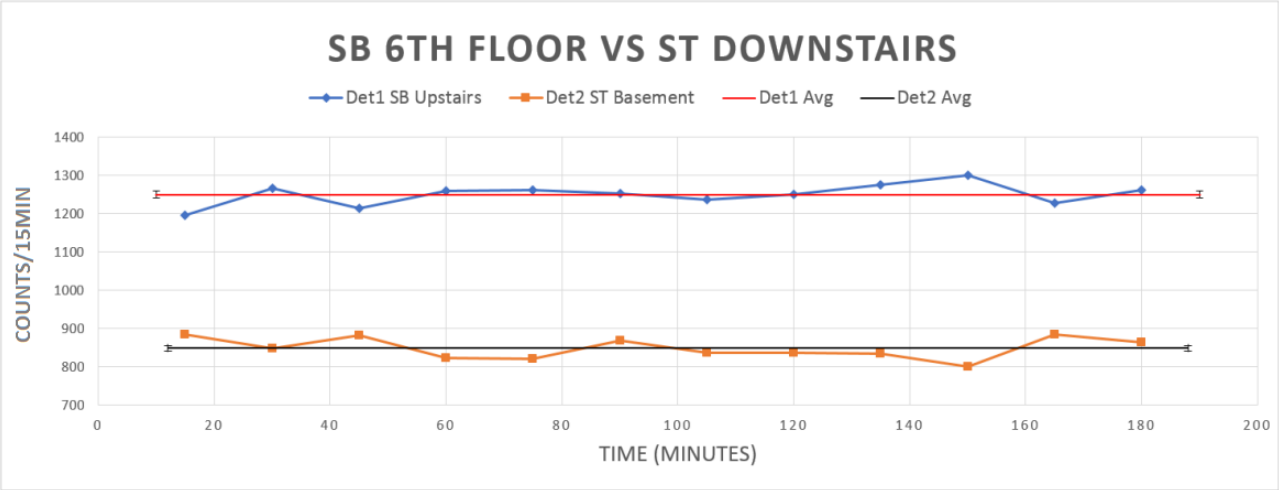

FIG. 16: First attempt at testing Einstein's theory of relativity by taking simultaneous counts at different elevations. Average count rates are shown by the straight lines.

$$N_0 = 15128 \pm 123, \quad N = 10276 \pm 101, \quad \frac{N}{N_0} = 0.679 \pm 0.009.$$

The cause for why there is a discrepancy between the counts was thought to be due to where the detectors were placed. The detector in upstairs SB was situated in a room with relatively little concrete above it, while the detector in downstairs ST likely had a considerable amount of concrete above it. The possibility of concrete attenuating incoming muons had been grossly underestimated, as studies have shown that just 1 meter of concrete blocks 33% of incident muons [13]. Therefore with even with 1 meter of concrete above detector 2 in ST basement, the low counts that were measured can be explained.

To investigate this further, an experiment was then performed where the same detector was placed outside of Science Theatres, at the same elevation. The results of this are shown in Figure 17, which shows that there was a significant difference between the counts acquired. The average count rate (λ) for both cases are,

$$\lambda_{inside} = 0.94 \pm 0.01\,\mathrm{s}^{-1}, \quad \lambda_{outside} = 1.32 \pm 0.01\,\mathrm{s}^{-1}, \quad \frac{\lambda_{inside}}{\lambda_{outside}} = 0.72 \pm 0.02$$

Comparing these values to the Cosmic Ray Shielding Data for concrete [13], there is approximately 0.9 m of concrete above the ST basement physics workroom.

With the knowledge that concrete was attenuating muons in the basement, the detector was brought outside to the metal chicken statue in front of the Science A building. Both

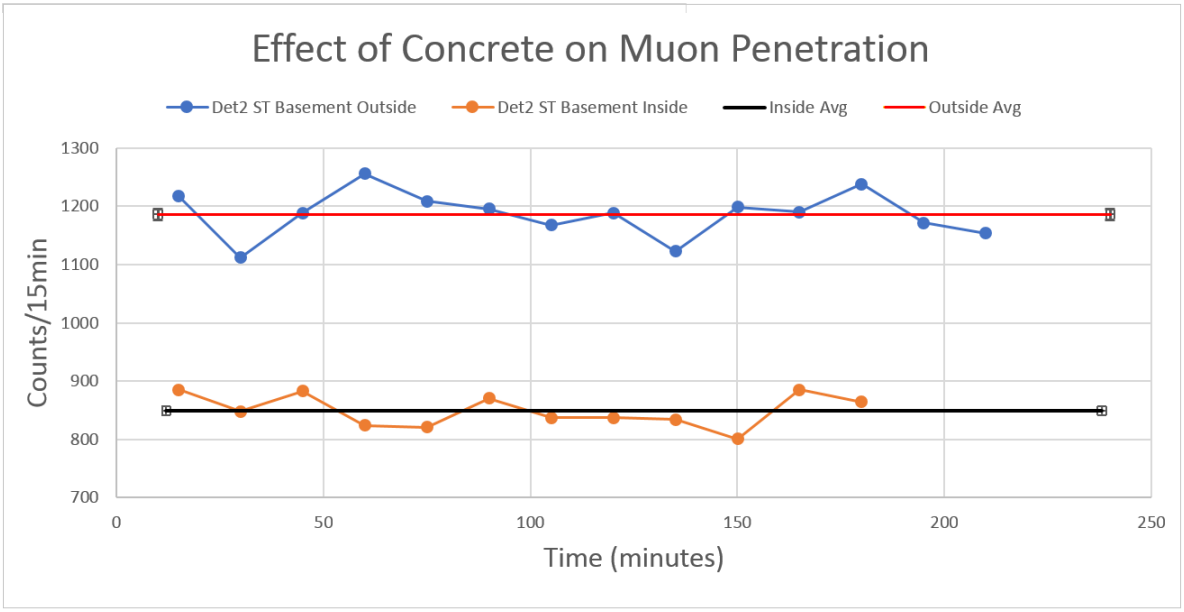

FIG. 17: Test of concrete's effect on muon count rates. Comparing this data to Concrete Shielding Data [13] this test suggests that there is around 0.9 meters of concrete above the undergradute physics workroom.

detectors were then set to collect data with no obstructions above them. The results from this experiment are shown in Figure 18.

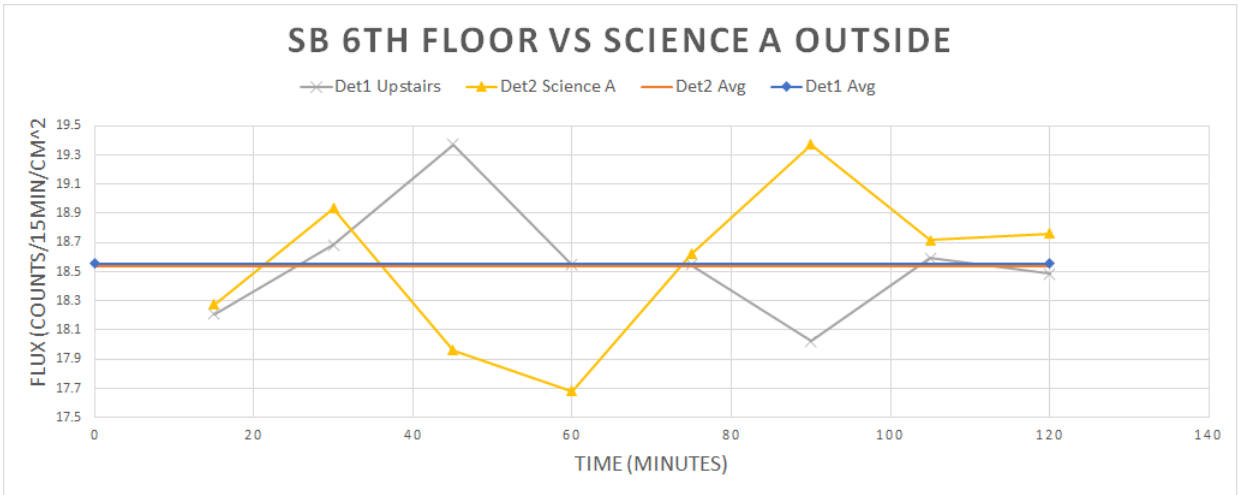

FIG. 18: Second test of Einstein's theory using two muon detectors at different elevations.

Over the course of 2 hours, a flux of $\Phi_{up} = (20.6 \pm 0.2) \times 10^{-3}$ count/sec/cm^2 was acquired for upstairs Science B, while a flux of $\Phi_{down} = (20.6 \pm 0.2) \times 10^{-3}$ count/sec/cm^2 was also acquired outside of Science A. The exact height difference is unknown between these points, but is estimated to be $h = 20 - 30$ m. The speed of the muons is assumed to be

$v = 0.994c$. Given these values along with that of Φ_{up}, classical theory predicts Φ_{down} to be: (Eq.5) $\Phi_{class.,20\text{m}} = 20.0 \times 10^{-3}$ count/sec/cm^2 to $\Phi_{class.,30\text{m}} = 19.7 \times 10^{-3}$ count/sec/cm^2 and relativistic theory predicts Φ_{down} to be (Eq.7) $\Phi_{rel.,20\text{m},30\text{m}} = 20.5 \times 10^{-3}$ count/sec/cm^2.

The measured flux from this experiment agrees with the relativistic prediction while also remaining larger than the classical prediction. Therefore it was shown that the relativistic theory must be used in making predictions of muon flux differences on Earth as predicted in Section IIA. This result could be made more accurate by performing an experiment using a larger height difference, such as on the top of a nearby mountain, and by taking data for a longer period of time.

VI. CONCLUSION

The development of desktop muon detectors was overall quite successful. The final products were in correspondence with the project goal; two small detectors that are extremely mobile and able to detect cosmic muons. Valuable lessons were learned in instrument development, time management for a long project, calibration, and experimentation. Early experiments with the detectors showed the influence of concrete on muon shielding. Relativistic theory was put to the test, with a positive result within error.

Future use for these detectors will most likely be educational in nature. They will be presented at the Canadian Nuclear Society's Annual Conference, showcasing their effectiveness in communicating ideas of cosmic radiation. The detectors could also be used effectively in a classroom or public demonstration as a way to educate people about particle physics, detectors, and radiation.

VII. ACKNOWLEDGEMENTS

I would like to thank my supervisor Dr. Jason Donev, as well as Wesley Ernst, Pat Irwin, and Dr. Chris Cully for graciously providing equipment and valuable input to my project. I'd also like to thank the Canadian Nuclear Society for their partial funding of this project.

[1] Written in the style of Phys. Rev. Letters in correspondence with “Physical Review Letters’ Style and Notation Guide”.

[2] S. Axani, J. Conrad, and C. Kirby, “The Desktop Muon Detector: A simple, physics-motivated machine- and electronics-shop project for university students," (June 2016).

[3] J. Beringer *et al.* (Particle Data Group), Phys. Rev. D 86, 010001 (2012).

[4] Figure 1 via Wikimedia Commons [Online], Available: https://upload.wikimedia.org/wikipedia/commons/thumb/0/08/Atmospheric_Collision.svg/2000px-Atmospheric_Collision.svg.png

[5] B. Rossi and N. Nereson “Experimental Determination of the Disintegration Curve of Mesotrons”. *Physical Review*. **62** (9-10): 417-422. doi:10.1103/PhysRev.62.417.

[6] N. Easwar and D.A. MacIntire. “Study of the effect of relativistic time dilation on cosmic ray muon flux - An undergraduate modern physics experiment.” Am. J. Phys 59.7 (1991): 589-592

[7] United Nations Scientific Committee on the Effects of Atomic Radiation, “Sources and effects of ionizing radiation” in *UNSCEAR 2008 Report*. New York: United Nations (published 2010). Available: http://www.unscear.org/docs/publications/2008/UNSCEAR_2008_GA-Report-CORR.pdf

[8] W.R. Leo, “The Poisson Distribution,” in *Techniques for Nuclear and Particle Physics Experiments*. Berlin, DE: Springer-Verlag, 1987, ch.4, sec.2.2, pp.79-80.

[9] W.R. Leo, “Scintillation Detectors,” in *Techniques for Nuclear and Particle Physics Experiments*. Berlin, DE: Springer-Verlag, 1987, ch.7, pp.149-167.

[10] SensL, “MicroFC-60035-SMT” [Online], Available: http://sensl.com/estore/microfc-60035-smt/

[11] Figure 6 via Wikimedia Commons [Online], Available: https://commons.wikimedia.org/wiki/File:Op-Amp_Non-Inverting_Amplifier.svg

[12] D.J. Griffiths, “Introduction to Electrodynamics", 4th ed. Upper Saddle River, USA: Pearson, 2013.

[13] E. Aguayo *et al.*, “Cosmic Ray Interactions in Shielding Materials", United States Department of Energy, prepared by Pacific Northwest National Labs, 2011.

Appendix A: Parts

Parts list for one detector
MicroFC 60035 Silicon Photomultiplier x1
0.96″ OLED display x1
1590C Aluminum box x1
Arduino Nano x1
Plastic scintillator block
Main/SiPM circuit board
5V DC power supply wall plug x1
DC Power Jack Socket 2.1mm x 5.5mm Barrel-Type x2
DC power cord with wire x1
BNC cable x1
BNC female connector x2
LT6201CS8 165MHz, Ultra Low Noise, RR OpAmp x1
Capacitors: 10 uF x3 .1 uF x1 10 nF x3 1 nF x1
Resistors (in Ohms): 49.9 x3 1k x3 10k x1 57.6k x1 100k x2
Schottky diode x2
Wires
Drill with various screws, nuts, and washers
Solder and solder paste

Appendix B: Code

This code is taken with permission from [2]. It is uploaded to the Arduino. I have taken the time to go through and understand it fully.

```
/*
Desktop Muon Counter Arduino Code
Questions?
Spencer N. Axani
saxani@mit.edu
Requirements: Sketch->Include->Manage Libraries:
  1. Adafruit GFX Library -- by Adafruit Version 1.0.2
  2. Adafruit SSD1306     -- by Adafruit Version 1.0.0
  3. Wire                 -- by Arduino Version 1.0.0
  4. OzOLED               -- Version unknown, can be found on github.
  5. SPI                  -- by Arduino Version 1.0.0
  6. TimerOne             -- by Jesse Tane et al. Version 1.1.0
*/

#include <Adafruit_GFX.h>
#include <Adafruit_SSD1306.h>
#include <Wire.h>
#include <OzOLED.h>
#include <SPI.h>
#include <TimerOne.h>

const int OLED = 0;               // Turn on/off the OLED [1,0] (Set to 0 to improve deadtime)
const int LED  = 0;               // Turn on/off the LED delay [1,0] (Set to 0 to improve deadtime)

//INTERRUPT SETUP
#define TIMER_INTERVAL 1000000     // Every 1,000,000 us the timer will update the clock on the OLED
```

```
//OLED SETUP
#define OLED_RESET 10              // A signal to this pin will reset the OLED screen
Adafruit_SSD1306 display(OLED_RESET);

//Linear regression parameters
float x1,x2,x3,x4,x5,x6;
float y1,y2,y3,y4,y5,y6;

float Sx2y,Sylny,Sxy,Sxylny,Sy;
float a, b;

//Timing variables
long measurement_t1  = 0L;                // Time stamp
long measurement_t2  = 0L;                // Used to calculate deadtime of signal measurement

long OLED_t1         = 0L;                // Used to calcualte deadtime of OLED screen update
long OLED_t2         = 0L;                // Used to calcualte deadtime of OLED screen update

long OLED_deadtime        = 0L;           // Tallies the OLED deadtime
long measurement_deadtime = 0L;
long total_deadtime       = 0L;

const float TIME_INTERVAL      = 5.8;     // Using a prescaler of 4, the time between analogue samples i

String      hist = "Initializing...";    // A histogram

const float SIGNAL_THRESHOLD  = 140;        // Signal threshold,
measured from 0-1023. Measuring from 0 to 300mV. 70 corresponds to
approximately 20 mV threshold.
const int   LED_PIN           = 3;         // The LED digital pin connections.
long int    count             = -1L;       // A tally of the number of muon counts observed
```

```
float SiPM_voltage     = 0;                  // This is the calculated
pulse amplitude of the SiPM signal
float signal_voltage   = 0;                  // This is the measured
signal amplitude from the pulse detector circuit

const String current_count_str  = "Total Count:";
const String runtime_str        = "Run Time:   ";
const String rate_str           = "Rate: ";
const String pm                 = "+/-";

long int time           = 0.;
int      seconds        = 0.;
int      minutes        = 0.;
int      hours          = 0.;
float    stdev          = 0.;
float    average        = 0.;
char     tmp2[15];
char     tmp[15];
String   current_count;
String   runtime;
String   rate;

void setup() {
Serial.begin(9600);

ADCSRA &= ~(bit (ADPS0) | bit (ADPS1) | bit (ADPS2));    // clear prescaler bits
ADCSRA |= bit (ADPS1);                                   // Set prescaler to 4

 display.begin(SSD1306_SWITCHCAPVCC, 0x3C);              // OLED screen
 display.clearDisplay();
```

```
if (OLED == 1){
  display.setTextSize(1);
  display.setTextColor(WHITE);
}

pinMode(LED_PIN, OUTPUT);                                    // Setup the LED pin to output

Timer1.initialize(TIMER_INTERVAL);                           // Initialise timer 1
Timer1.attachInterrupt(timerIsr);                            // attach the ISR routine

getTime();
}
void loop() {
  while (1) {
    if (analogRead(A0) > SIGNAL_THRESHOLD) // If true, we have an event!
        {
        y2 = analogRead(A0);              // Read analogue pin A0 five times.
        y3 = analogRead(A0);
        y4 = analogRead(A0);
        y5 = analogRead(A0);
        y6 = analogRead(A0);

        total_deadtime += measurement_deadtime + OLED_deadtime;
        // time_pulse == deadtime of previous measuremnet. time_oled
        == deadtime associated with updating clock.

        measurement_t1 = millis();        // Time stamp of event

        noInterrupts();                   // Turn off the interupts, so that it doesn't update
        the OLED screen mid measuremnt
        x1 = 0;                           // This is the time of the first measurement: y1
```

```
x2 = x1 + TIME_INTERVAL + 0.5;    // It takes 504ns to perform the IF statement
x3 = x2 + TIME_INTERVAL;
x4 = x3 + TIME_INTERVAL;
x5 = x4 + TIME_INTERVAL;
x6 = x5 + TIME_INTERVAL;
digitalWrite(LED_PIN, HIGH);          // Turn on the LED

// Calculate the initial pulse amplitude. This is just a exponential regression fit.
Sx2y   = x2*x2*y2 + x3*x3*y3 + x4*x4*y4 + x5*x5*y5 + x6*x6*y6;
Sylny  = y2*log(y2) + y3*log(y3) + y4*log(y4) + y5*log(y5) + y6*log(y6);
Sxy    = x2*y2 + x3*y3 + x4*y4 + x5*y5 + x6*y6;
Sxylny = x2*y2*log(y2) + x3*y3*log(y3) + x4*y4*log(y4) + x5*y5*log(y5) + x6*y6*log(y6);
Sy     = y2 + y3 + y4 + y5 + y6;

a = (Sx2y*Sylny - Sxy*Sxylny) / (Sy*Sx2y - Sxy*Sxy);
b = (Sy*Sxylny - Sxy*Sylny) / (Sy*Sx2y - Sxy*Sxy);
y1 = exp(a);                          // y1 is the calculated amplitude of the
triggering pulses at the time of the trigger.


signal_voltage = y1 * 5./1023.;    // Convert the measured value,
y1 , to a voltage (0-1024 == 0-5V)
count++;                           // Increment the number of counts

float aa = -0.0000213241;    // These numbers come from the calibration of the electronics.
float bb =  0.0236566939;
float cc = -(0.3378053306 + signal_voltage);
SiPM_voltage = (-bb + sqrt(sq(bb) - 4*aa*cc))/(2*aa);
if (count > 0){
  Serial.println((String)count + " " + (String)measurement_t1 + " " + (String)signal_voltage + "
}
```

```
        interrupts();                       // Allow for interupts, to update OLED

        if (LED == 1){
          delay(signal_voltage*500);}
        digitalWrite(LED_PIN, LOW);            // Turn off the LED

        measurement_t2 = millis();
        measurement_deadtime = measurement_t2 - measurement_t1;
        OLED_deadtime = 0;
        }
    }
}
//TIMER INTERUPT
void timerIsr(){
interrupts();
if (OLED == 1){
  getTime();}
noInterrupts();
}
//UPDATE OLED SCREEN. It takes approximately 33ms to run the getTime function
void getTime(){
  OLED_t1 = millis();
  if (signal_voltage > 0.0)   {hist = "-";};
  if (signal_voltage > 0.2)   {hist = "--";};
  if (signal_voltage > 0.4)   {hist = "---";};
  if (signal_voltage > 0.6)   {hist = "----";};
  if (signal_voltage > 0.8)   {hist = "-----";};
  if (signal_voltage > 1.0)   {hist = "------";};
  if (signal_voltage > 1.2)   {hist = "-------";};
```

```
if (signal_voltage > 1.4)   {hist = "--------";};
if (signal_voltage > 1.6)   {hist = "---------";};
if (signal_voltage > 1.8)   {hist = "----------";};
if (signal_voltage > 2.0)   {hist = "-----------";};
if (signal_voltage > 2.2)   {hist = "------------";};
if (signal_voltage > 2.4)   {hist = "-------------";};
if (signal_voltage > 2.6)   {hist = "--------------";};
if (signal_voltage > 2.8)   {hist = "---------------";};
if (signal_voltage > 3.0)   {hist = "----------------";};
if (signal_voltage > 3.2)   {hist = "-----------------";};
if (signal_voltage > 3.4)   {hist = "------------------";};
if (signal_voltage > 3.6)   {hist = "-------------------";};
if (signal_voltage > 3.8)   {hist = "--------------------";};
display.setCursor(0, 0);
time                = millis() / 1000.;
seconds             = time    % 60;
minutes             = time / 60 % 60;
hours               = time / 3600;
stdev               = sqrt(count) / (time-total_deadtime/1000.);
average             = (float)count / (time-total_deadtime/1000.);
display.clearDisplay();
current_count        = current_count_str + " " + count ;
runtime             = runtime_str + hours + ":" + minutes + ":" + seconds;
dtostrf(average, 1, 3, tmp);
if(stdev <= 0.001){
  char a = 0.000;
  dtostrf(a, 1, 3, tmp2);
}
else{
  dtostrf(stdev, 1, 3, tmp2);
}
```

```
  rate = rate_str + tmp + " " + pm + " " + tmp2;
  display.println(current_count);
  display.println(runtime);
  display.println(hist);
  display.println(rate);
  display.display();
  //Serial.println(rate);
  OLED_t2 = millis();
  OLED_deadtime += (OLED_t2-OLED_t1);
}
```